Published in final edited form as:
Hear Res. 2010 April ; 262(1-2): 45–55. doi:10.1016/j.heares.2010.01.008.

γ-Aminobutyric acid is a neurotransmitter in the auditory pathway of oyster toadfish, *Opsanus tau*

Peggy L. Edds-Walton[a,b], **Gay R. Holstein**[a,c], and **Richard R. Fay**[a,b]

[a]Neuroscience Institute, Marine Biological Laboratory, 7 MBL St., Woods Hole, MA 02543 USA

[b]Parmly Hearing Institute, 6525 North Sheridan Rd, Loyola University, Chicago, IL 60626 USA

[c]Departments of Neurology and Neuroscience, Mount Sinai School of Medicine, New York, NY 10029 USA

Abstract

Binaural computations involving the convergence of excitatory and inhibitory inputs have been proposed to explain directional sharpening and frequency tuning documented in the brainstem of a teleost fish, the oyster toadfish (*Opsanus tau*). To assess the presence of inhibitory neurons in the ascending auditory circuit, we used a monoclonal antibody to GABA to evaluate immunoreactivity at three levels of the circuit: the first order descending octaval nucleus (DON), the secondary octaval population (dorsal division), and the midbrain torus semicircularis. We observed a subset of immunoreactive (IR) cells and puncta distributed throughout the neuropil at all three locations. To assess whether contralateral inhibition is present, fluorescent dextran crystals were inserted into dorsal DON to fill contralateral, commissural inputs retrogradely prior to GABA immunohistochemistry. GABA-IR somata and puncta co-occurred with retrogradely filled, GABA-negative auditory projection cells. GABA-IR projection cells were more common in the dorsolateral DON than in the dorsomedial DON, but GABA-IR puncta were common in both dosolateral and dorsomedial divisions. Our findings demonstrate that GABA is present in the ascending auditory circuit in the brainstem of the toadfish, indicating that GABA-mediated inhibition participates in shaping auditory response characteristics in a teleost fish as in other vertebrates.

Keywords

auditory processing; descending octaval nucleus; inhibition; directional hearing; secondary octaval nucleus

Introduction

The male oyster toadfish (*Opsanus tau* L., Batrachoididae) advertises the location of his nest site vocally to attract reproductive females (Gray and Winn, 1961; Fish, 1972). The females approach the nest site, interact with the male, and eventually deposit their eggs for fertilization. In addition to attracting females, the reproductive “boatwhistle” sound of one male can stimulate boatwhistles from other males in the area (Winn, 1967; Fish, 1972). Therefore,

Corresponding Author address: Dr. PL Edds-Walton, Marine Biological Laboratory, 7 MBL St., Woods Hole, MA 02543 USA, plewalton@yahoo.com.

hearing and sound source localization are important for successful reproduction, and the toadfish is an appropriate species in which to evaluate the components of the auditory circuit that may contribute to sound source localization in a teleost fish.

A substantial amount of information has been learned about the auditory pathway in the toadfish. The ear of the oyster toadfish (Edds-Walton and Popper, 1995) is similar to the ear of other teleost fishes that are not specialized for pressure reception (Popper and Fay, 1999), and the auditory pathway is consistent with that of other nonspecialists (McCormick, 1999). The auditory hair cells on the saccule, an otolithic endorgan, encode the frequency content and direction of the particle motion component of underwater sounds below about 300 Hz (Fay and Edds-Walton, 1997). The axons of primary auditory afferents innervating the saccule branch centrally to provide inputs to multiple sites along the rostro-caudal extent of the ipsilateral descending octaval nucleus (DON) (Edds-Walton et al., 1999). Although not clearly delineated anatomically, functional subdivisions have been demonstrated in the DON of toadfish: auditory processing occurs in the dorsal portion of the nucleus (Edds-Walton et al., 1999; Edds-Walton and Fay, 2008), whereas vestibular processing occurs more ventrally (Highstein et al., 1992; Mensinger et al., 1997). Moreover, tract-tracing studies combined with physiological recordings in the auditory midbrain have confirmed that a subset of cells in the ipsilateral and contralateral dorsal DON of the toadfish project to the auditory midbrain (torus semicircularis, TS)(Edds-Walton and Fay, 2003), along with ipsilateral and contralateral projections from secondary octaval populations. These anatomical data are consistent with other teleost fishes in which similar studies have been conducted (McCormick, 1999).

Physiological studies of response characteristics in the DON and TS of toadfish have revealed components of auditory processing related to encoding frequency and the direction of a sound source. In comparison to the response areas of primary afferent fibers, both frequency tuning (narrower response area to the stimulus frequencies) and directional sharpening (narrowing of the response area to directional particle motion, defined in Fay and Edds-Walton, 1999) have been documented among auditory cells in the DON and the midbrain of *O. tau* (Edds-Walton and Fay, 2003, 2005a, 2008). In the DON, approximately 60% of the cells exhibit directional sharpening, while 40% exhibit directional responses that are like those of primary afferents (Edds-Walton and Fay, 2005a). The primary-like directional responses of a subset of DON cells may be critical functionally for the sharpening that occurs in the nucleus. Directional sharpening in the DON can be modeled as the “sum” of the response areas from two primary afferent-like directional inputs of opposite sign with different best axes (one excitatory and one inhibitory) converging on a DON cell (Fay and Edds-Walton, 1999). Interneurons in the DON may provide the sign reversal (inhibition) necessary for this additive process to yield sharpened directional responses. Alternatively or additionally, commissural projections from contralateral DON cells (Edds-Walton, 1998) could provide inhibitory inputs that result in directional sharpening. Contralateral inputs are necessary to obtain the entire range of best directions documented in the DON (Edds-Walton and Fay, 2009).

Horner et al. (1980) provided the first physiological evidence that binaural auditory processing occurs in the brainstem of a teleost (cod, *Gadus morhua*). More recent research with the toadfish has shown that contralateral input can be either excitatory (E) or inhibitory (I) and that binaural EI, IE, and EE cells in the DON and TS contribute to the directional responses (Edds-Walton and Fay 2009). These findings are particularly notable since, in most other vertebrates, binaural cells are not present in the first order auditory nucleus, but rather occur in a specialized secondary octaval nucleus, e.g., the nucleus laminaris in birds, and nuclei of the superior olive in mammals (see review in Grothe et al. 2004).

Identification of the neurotransmitters mediating binaural responses in toadfish will permit further physiological assessment of the computations occurring in the ascending auditory

pathway of fish. Gamma aminobutyric acid (GABA) is a common inhibitory neurotransmitter in vertebrates, and GABA-mediated inhibition has been shown to be important in shaping response properties along the pathways involved in sound source localization in birds and mammals, though not in identical ways (Hyson et al. 1995) and at different levels of the pathway (see review in Grothe et al. 2004).

In birds and mammals, two parallel pathways begin with the projections from the nucleus (or nuclei) that receive primary auditory inputs. One pathway encodes timing information required to compute the interaural time difference (ITD) while the other encodes sound level for the interaural intensity difference (IID). The interaural difference cues available to terrestrial vertebrates are not likely to be available to teleost fishes due to (1) the proximity of the ears, (2) the higher density of water, which means that sound travels about five times faster in water than in air (fish tissue is approximately the same density as the surrounding water), and (3) best frequencies below 500 Hz for most fish (Fay, 2005). Thus the interaural time differences for a fish would be 1/5 those in air for a terrestrial vertebrate with similarly small interaural distances, and the wavelengths of sounds in the best frequency range (> 3m) would not provide detectable interaural phase differences. Therefore, the detection of interaural differences for sound source localization by fishes must be based on computations that differ in some way from those in terrestrial mammals. However, the same inhibitory neurotransmitters common to other vertebrate sensory systems may be used in the ascending circuit that computes sound location in fishes.

GABAergic inhibition plays a role in both the ITD and the IID pathways of birds (e.g., Bruckner and Hyson, 1998; Carr et al., 1989; Funabiki et al. 1998; Hyson, 2005; Muller, 1987; Konishi, 2003), and in the IID pathway of mammals, which may be more important than ITD for sound localization in some terrestrial mammals with small heads, such as bats (Klug et al. 1995; Park and Pollak, 1993, 1994; Pollak et al., 2002, 2003).

The present study was undertaken to determine whether GABAergic neurons or inputs are present in auditory processing sites in the DON and/or are associated with projection cells and nuclei in the ascending auditory pathway to the midbrain. This study represents a first step in evaluating whether GABA plays a role in shaping the directional response characteristics of auditory cells in the brainstem of the toadfish.

Materials and methods

Anatomy

Previous work has identified the approximate borders of the DON in the oyster toadfish, *O. tau* (Highstein et al., 1992; Edds-Walton et al., 1999; Edds-Walton and Fay, 2003, 2005a,b, 2008). As in all fishes, there are no distinct borders that define the octaval nuclei, rather, there are assemblages of cells that have been defined primarily based on cytology and connectivity (McCormick 1999; see figure 1). The anatomical terminology used herein corresponds to that used in our previous publications, which is consistent with the detailed description of the toadfish octaval column by Highstein et al. (1992), but also includes the dorsolateral and dorsomedial auditory divisions of the DON described in the midshipman (*Porichthyes notatus*, Batracoididae) and *O. beta* (the Gulf toadfish) by Bass et al. (2000, 2001). In *O. tau*, the dorsolateral DON (DONdl), is present above the descending tract of the trigeminal (V_{desc}) and is largest near the entrance of cranial nerve VIII. The ventrolateral DON (DONvl) is located at the lateral edge adjacent to and ventral to V_{desc} (Fig. 1). DONdl and DONvl subdivisions become indistinct as DON diminishes along the lateral edge of the medulla (Highstein et al. 1992). The dorsomedial DON (DONdm) in *O. tau* begins in the region of the entrance of VIII, and co-occurs rostrally with the dorsal nucleus of the secondary octaval

population (SOdor). Cells in DONdm usually have processes that extend both laterally and/or dorsally (see neurobiotin-filled cells in figure 1A,B).

The DON receives input from all the endorgans innervated by the anterior and posterior rami of the VIIIth nerve. Central projections of physiologically characterized primary afferents have confirmed that vestibular projections are concentrated in the ventrolateral area around V_{desc} (Mensinger et al., 1997) and saccular auditory projections extend throughout the dorsal DON (Edds-Walton et al., 1999). Auditory responsiveness has been confirmed physiologically in both DONdl and DONdm, with no obvious regional differences revealed thus far (Edds-Walton and Fay, 1998, 2005a,b, 2008). The term *dorsal DON* will be used herein to include the subdivisions of DONdm and DONdl when they are not referred to separately.

For all surgical procedures the gills of the fish were washed with buffered tank water containing MS222 (3-aminobenzoic acid methane-sulfonate salt, 1:1000 seawater buffered with $NaHCO_3$, pH 7.4) until gilling activity ceased. Adult fish (15 – 24 cm standard length) were paralyzed with a 0.1 - 0.2 ml intramuscular injection of pancuronium bromide (1mg/ml solution in 0.1M standard phosphate buffer with 0.9% NaCl) and placed in a Plexiglas enclosure with aerated sea water. Lidocaine was applied topically to the skin with a Q-tip, a rectangular incision was made dorsally, and the skin was reflected caudally to reveal the dorsal muscles. The muscle over the skull was removed and the bone thinned with a dental scraper to allow gentle removal of the bone and exposure of the brain. Intracranial fluids were replaced with a fluorocarbon plasma substitute (FC-77, 3M Corp.) to provide a clearer view of the brain.

Neurobiotin or a fluorescent dextran amine (Molecular Probes/Invitrogen) were used to label the somata and processes of cells in the DON. Neurobiotin had been used to label recording sites during previous physiological studies of the DON (see Fay and Edds-Walton, 1999; Edds-Walton and Fay 2005a,b, 2008) and some of that tissue was re-analyzed for this study (n = 10 fish). The fluorescent dextran amine was used alone in a preliminary study to assess transport time to fill contralateral cells (n = 2 fish) and in conjunction with GABA immunohistochemistry to identify GABAergic contralateral projection cells in the DON as described in detail below (n = 4 fish).

Neurobiotin (4% in 1-2M NaCl) was injected from the recording electrode at an electrophysiologically confirmed auditory site in the dorsal DON via positive current (1600 – 2000 nAmps) for 20-30 min with a 50% duty cycle (1 sec on, 1 sec off) to obtain extensive labeling of DON cells. Details of the electrophysiology may be found in Edds-Walton and Fay (2008). The surgical opening was closed with gelfoam (UpJohn); the skin flap was replaced and sealed with parafilm. The fish was placed in aerated seawater for label transport to occur over 8 – 12 hrs at 12° C. The toadfish then was anesthetized again (as above) and perfused through the heart with toadfish saline (160 mM NaCl, 4mM KCl, 82 mM sucrose) in 0.1M standard phosphate buffer (PB, pH 7.4) followed by perfusion with fixative (4% paraformaldehyde in buffered toadfish saline). The brain was excised and postfixed for 1 hr, rinsed, and refrigerated in 0.1M PBS (PB with 0.9% NaCl) overnight.

The brain was cryoprotected by infusion of 40% sucrose (in 0.1M PBS) for 24 hrs. The brain was then embedded in Tissue-Tek (OTC), allowed to freeze for 20 – 30 min at -24°C in the cryostat (Microm HM 505M), and sectioned transversely (50 μm). The neurobiotin was visualized in floating sections using a standard ABC-DAB reaction (Molecular Probes, Elite kit) with metal intensification (solutions in Hancock, 1982) and incubation times determined visually (10 – 30 min) to minimize background staining. The sections were stored in buffer (0.1M PB) until mounted onto gelatin-coated slides, dehydrated through alcohols, cleared in Citrisolv (Fisher), and cover-slipped for examination on an Olympus BX50 microscope with drawing tube and digital camera (DP12 camera system). Cell morphology and measurements

(maximum length and perpendicular width) were obtained at 400× while using a scale viewed simultaneously through the drawing tube. The scale (1 μm resolution) was drawn from a slide micrometer (FST, Inc.) viewed at the same magnification (400×).

The fluorescent tetramethyl rhodamine dextran (TMR-dextran: anionic, lysine-fixable, 3,000 MW; Molecular Probes) was used to label dorsal DON sites to reveal projection cells in the contralateral DON. The efficacy of the method was evaluated prior to use of the TMR-dextran in conjunction with the GABA antibody (detailed below). Crystals of TMR-dextran were inserted dorso-laterally on a minutin pin into the left DON dorsal to the entrance of VIII to ensure uptake in the dorsal, auditory divisions. The use of crystals results in a greater number of labeled somata than iontophoresis of TMR dextran in solution (personal observations). After 5 min, the brain area was rinsed twice with toadfish saline, and the opening of the skull was closed as described above. Incubation times and procedures for tissue preparation were as above except for visualization of the label. The sections were placed on acid-washed slides, covered with ProLong (Molecular Probes), and viewed on a Zeiss AxioImager (Z1) in the Marine Biological Laboratory Microscopy Facility with appropriate filters and photographed with a CamMR monochrome digital camera in grayscale or pseudocolor (red for TMR dextran) in tissue with two fluorophores (see below). Following confirmation of TMR-dextran transport to contralateral projection cells, this protocol was also used to prepare tissue for co-localization of GABA immunoreactivity among projection cells in DON.

Immunohistochemistry

A monoclonal GABA antibody (MAb GABA93) produced in the Holstein laboratory (Holstein et al., 2004a) was used for two aspects of this study. First we determined the distribution of GABA immunoreactive (GABA-IR) cells, processes, and puncta in the auditory medulla and midbrain (n = 3 fish). Secondly, we utilized the antibody to visualize the distribution of GABA immunoreactivity among projection cells in the DON that were labeled with TMR dextran (see above). Tissue preparation was as above, except that the fixative included 0.25% glutaraldehyde in addition to the 4% paraformaldehyde in 0.01M PBS. Initially 50 μm coronal sections were used (obtained as described above); subsequently, three brains were sectioned at 25 μm (1 coronal; 2 horizontal) with the same protocol.

Antibody specificity was demonstrated previously using enzyme-linked immuno-sorbent assays (ELISA) and was used successfully in the vestibular system of *O. tau* in a prior study (Holstein et al., 2004a,b). For the present study, we incubated medullary sections in NGS buffer (5% normal goat serum with 0.05% Triton X-100 in 0.01 M PBS) without the primary antibody, followed by incubation with the secondary antibody to control for nonspecific binding of the secondary reagent. As expected, no label was present in the control tissue. Positive controls for tissue processing included sections of the cerebellum, in which GABA-IR was consistently observed in Purkinje cells.

The protocol to visualize GABA immunopositive sites was modified from that of Holstein et al. (2004a). The floating sections were washed three times with 0.01M PBS and then immersed in NGS buffer overnight at room temperature. The sections were incubated at room temperature for 24 hrs in the primary antibody (GABA93 MAb) that had been diluted in NGS buffer (ratio of 1:20 or 1:30). The tissue was rinsed six times (10 min each) in 0.01 M PBS, immersed in NGS buffer for 1 hr, and then incubated with a fluorescent secondary antibody (goat anti-mouse IgG1 AlexaFluor dyes; Invitrogen) in the NGS buffer (2 μg/ml) for 6 hr at room temperature while covered with aluminum foil on a gyratory table in minimal room illumination. The secondary antibody was red-fluorescing Alexa 594 (emission maximum 617 nm) for the first set of experiments in which we determined the distribution of GABA immunoreactivity. Green-fluorescing Alexa 488 (emission maximum 521nm) was employed as the secondary for all double-label experiments in which red TMR-dextran was used to visualize cells in DON.

Immunoreacted sections were rinsed six times (10 min each) in 0.01 M PBS before mounting on acid-washed slides in ProLong (Molecular Probes).

The immunoreacted tissue was examined on a Zeiss AxioImager using high efficiency filter sets (38 HE, 43HE) with a CamMR monochrome camera (Marine Biological Laboratory) and the min/max option to maximize the value range with appropriate pseudo-color to distinguish the two fluorophores. Some of the tissue was also reviewed and photographed on a Leica DMRE fluorescence microscope (Federicci Lab, UC Riverside) with appropriate filters and pseudocolor.

The care of the toadfish and our experimental procedures were approved by the Animal Care and Use Committees of the Marine Biological Laboratory and Loyola University Chicago. Annual reviews of the protocols were conducted at the MBL, where the fish were obtained, held, and used during this study.

Results

Cell morphologies

Neurobiotin iontophoresed into physiologically identified auditory sites in the left, dorsal DON provided substantial numbers of filled somata ipsilaterally in 10 toadfish (range of ipsilateral DON cells in each fish: 13 – 41) and contralaterally in 8 of those fish. The contralateral data will be presented in the next section. Most of the neurobiotin injections were in DONdl. The injection size and incubation time resulted in considerable uptake and transport of the neurobiotin into somata and their processes along both the rostral-caudal and lateral-medial axes. Lateral processes of the cells in DONdm (as in figure 1A,B) took up neurobiotin and filled somata were present in the ipsilateral DONdm in all fish, though in varying numbers. Out of the 233 cells filled sufficiently for categorization, 129 were in DONdl and 104 were in DONdm. Retrogradely filled somata were seen ipsilaterally along the length of the DON, as far as 900 μm rostral or caudal to the site of neurobiotin deposition.

Neurobiotin-filled cells were categorized into one of six cell types based on (1) the apparent shape of the soma and (2) relative size and distribution of the processes as they appeared in a single coronal section (Fig. 2). Size of the soma was recorded as maximum length and perpendicular width, but the size ranges were overlapping for most of the cell types; therefore, size alone was not distinctive. No mathematical adjustments were attempted to compensate for tissue shrinkage during processing. No three-dimensional reconstructions were attempted, nor were axons and dendrites identified by their ultrastructure; however, the axons of commissural projection cells were distinguishable as they traveled medially to the internal arcuate tract. No filled somata without processes were included in the study, and only ipsilateral fills were used in these initial analyses (n = 233 cells in 10 fish).

The ranges of cell sizes (and mode for length, width) are given in Table 1 for comparative purposes. The entire volume of the soma and the associated processes may not have been visible, and the classification should be considered preliminary. Type 1 cells had a relatively small, round or oval soma with two narrow processes, usually opposed diametrically (Fig. 2). Type 2 was a fusiform cell with two large processes that were diametrically opposed on the long axis of the soma (Fig. 2). For some cells in this category, a small process, possibly the axon, was visible orthogonal to the long axis.

Type 3 cells had a conical or tear-drop shaped soma with a large dendrite directly opposed by a thin axon-like process that could often be traced to the region of the internal arcuate tract, indicating that these cells can be projection neurons (Fig. 2). Some cells classified as Type 3 also had a truncated orthogonal dendrite that may have traveled along the rostro-caudal axis

of the DON (not shown in illustration). The primary criterion for these cells was the single large dendrite extending from the long axis of the soma.

Type 4 cells were distinguished by the presence of two parallel processes emerging from the moderately sized soma (Table 1) and a single opposing process (Fig. 2). The morphology was very consistent, though rare. Type 5 cells had polygonal somata with two dendritic processes that were either oriented along the same axis or orthogonal to each other (Fig. 2). Type 5 cells were similar to the fusiform Type 2 cell, but they differed in that the soma of the Type 5 cell was always eccentric with respect to the axis of its major processes. Type 6 cells were multipolar, with relatively large somata (Table 1) and processes at a variety of orientations (Fig. 2).

The cell types were not equally distributed throughout the dorsal DON, although there were no regions dominated completely by a single cell type. Table 2 provides details of the proportions of each type seen in the dorsolateral (DONdl) and dorsomedial (DONdm) divisions of the DON. The greatest proportion of cells labeled in the DONdl were Type 3 (56/129 = 43%); however, in DONdm, the proportions of Types 3 and 2 were nearly equal (Table 2). Cells with Type 5 morphology were present as a greater proportion of the cells filled in DONdm than in DONdl. Types 4 and 6 were relatively uncommon in both divisions. Overall, the data indicate that there is a heterogeneous distribution of the six cell morphologies in the dorsal DON.

Although neurobiotin was never inserted into the secondary octaval population directly, SOdor somata were labeled ipsilaterally in two of the ten preparations (e.g., Fig. 1). In both cases, the label site in DONdl was in rostral DON, near the caudal border of the secondary octaval population. The label may have been picked up by lateral processes of the SOdor cells, although those processes were not distinguishable. Terminal boutons were apparent on and around the somata in the ipsilateral SOdor in several of the cases in which the SOdor somata themselves were not labeled by neurobiotin, suggesting input to SOdor from DON (data not shown).

Contralateral projection cells

After determining the cell types present ipsilaterally, retrogradely filled cells on the contralateral side were examined in detail to determine whether a particular DON cell type conveys commissural input. Cells in the contralateral (right) DON were labeled with neurobiotin through retrograde transport via their axons or axon collaterals in the left DON. For these analyses, we assumed that all cell morphologies were equally likely to transport neurobiotin retrogradely.

Label uptake was variable among the experimental fish (number of ipsilateral fills per fish: 13 – 38; number of contralateral fills per fish: 3 – 15). On average, the number of somata filled contralaterally was 20% of those filled ipsilaterally, but ranged from 5% to 59% of the number filled ipsilaterally. The variability was not unexpected because label sites were not identical among fishes as we attempted to survey the dorsal DON and determine the locations of projection cells. The filled axons of contralateral projection cells crossed the midline with the internal arcuate fibers and traveled along the medial boundary of the contralateral DON. Contralateral DON somata were filled along the length of the nucleus, indicating that the interconnections between the left and right DONs are extensive.

The commissural cells filled contralaterally were compared to the population of cell morphologies documented ipsilaterally (Figs. 3A,B). The ipsilateral data used for these comparisons differs from that in Table 2 because the data considered here are only from fishes with bilateral fills (n = 8 brains). The data are presented in figure 3A as the number of cells filled sufficiently on each side (*ipsi versus contra)*. Note that the relative occurrence of each

cell type seen contralaterally is similar to what was seen ipsilaterally, with the exception of Type 5, which was filled relatively more often ipsilaterally than contralaterally.

Although all cell types were represented among the filled cells contralaterally (Fig. 3A), Types 1 – 3 appear to be have the greatest involvement in the commissural pathway. We next examined the distribution of contralaterally filled Types 1 – 3 in the two subdivisions of DON (dl, dm) and compared those with the numbers of filled cells counted ipsilaterally (Fig. 3B). These data indicate that Types 1 - 3 are involved in a commissural auditory pathway in both DONdl and DONdm.

GABA immunoreactivity

In the second set of experiments, we evaluated GABA immunoreactivity in the auditory medulla and auditory midbrain using GABA93 MAb as the primary antibody and an Alexa 594-conjugated secondary reagent. Six brains were processed with slight variations in the protocol to minimize background and maximize tissue quality. Although all of the tissue demonstrated GABA immunoreactivity at auditory sites in the medulla and midbrain, the final four were most informative. The coronal series confirmed that GABA-IR somata were present in both the dorsal and ventro-lateral DON. The horizontal sections confirmed that GABA immunoreactivity was present along the entire length of the dorsal DON. GABA-IR profiles were also present in non-auditory areas of the medulla and midbrain, but those sites will not be described here.

GABA-immunolabeled cell bodies and puncta were present in both divisions of the dorsal DON, although GABA-IR somata were more common laterally than medially. The relative proportion of GABA-IR versus GABA-negative somata was not quantified since the total number of somata in each division within each fish could not be determined. Most of the GABA-immunolabeled cell bodies in the dorsal DON displayed Type 3 morphology (Figure 4A, lower arrow); other cells appeared to be of the Type 2 group, based on the fusiform shape of the somata. There were also scattered globular GABA-IR somata present in the region. GABA immunoreactive processes and puncta were prevalent in the neuropil and were often observed surrounding the somata of GABA-negative cell bodies in the dorsal DON (Fig. 4B). GABA-negative somata, lacking GABA-IR puncta, were present as well (upper left area of Fig. 4A).

The auditory efferent nuclei, which lie ventral to the medial longitudinal fasciculus at the midline, exhibited considerable GABA immunoreactivity (Fig. 4C). A range of immunoreactivity was present, with the brightest, most heavily immunoreactive cells located medially in the efferent nuclei. GABA-IR processes were also present, and they followed the pathway of efferent axons, which travel both laterally and across the midline.

GABA immunoreactivity was also documented in nuclei of the ascending auditory circuit. GABA appears to be present primarily in processes and puncta in the secondary octaval nucleus, SOdor, although a few of the SOdor somata were immunopositive (Figs. 5A, B). GABA immunoreactivity was present as scattered processes and puncta throughout the midbrain TS (nucleus centralis, NC, and nucleus ventralis, NVL)(Figs. 6A, B), and somata in the periventricular layer (pvc) that overlies the NC were heavily GABA-IR (Fig. 6A). Although processes of the cells in the periventricular layer extend ventrally through NC and NVL (Edds-Walton and Fay, 2005b), those processes could not be distinguished in this tissue. The labeling pattern among these brainstem nuclei suggests that GABAergic inhibition contributes to auditory processing at multiple sites along the ascending auditory pathway.

GABA and Commissural Cells in DON

The final series of experiments addressed the potential for inhibitory inputs among commissural projections using retrograde transport of the red-fluorescing TMR-dextran placed in the left, dorsal DON followed by reaction with the GABA93 MAb visualized with the green-fluorescing Alexa 488 secondary antibody (n = 4 brains). In all cases, cells lacking both TMR-dextran and GABA immunoreactivity were consistent with the background levels of fluorescence.

In all the experimental tissue, a subset of contralateral projection cells filled retrogradely with TMR-dextran were also GABA-IR (Figs. 7A-C). These double-labeled cells in DONdl provide evidence that contralateral inputs can be GABAergic. GABAergic puncta were present in the neuropil and were interpreted to be axonal varicosities and boutons. Some of these puncta were located in proximity to GABA-negative somata (long arrows, Fig. 7A) that were scattered among strongly GABA-IR somata (plus sign in Figs. 7A, B) and double-labeled somata (short arrows in Figs. 7A-C) in the contralateral DON. The GABA-IR somata that are not double-labeled may or may not project to the contralateral DON, given that retrograde transport of the TMR-dextran cannot be assumed to occur successfully for all projection cells in a population. However, it is clear that both GABA-IR and GABA-negative inputs are present in DONdl, and at least some of those inputs originate in the contralateral DON. Although the processes were rarely distinguishable for individual somata in this tissue, some of the GABA-IR somata in DONdl appeared to be tear-drop, Type 3 cells or small Type 1 cells.

GABA-IR somata were less common in DONdm than DONdl, although GABA-IR processes and puncta were present as in DONdl. Confirmed projection cells in the right DONdm (retrogradely filled with TMR-dextran placed in the left DON) exhibited numerous GABA immunoreactive puncta associated with the somata and processes (Figs. 8A-C). An array of GABA-IR puncta are apparent in proximity of a GABA-negative soma of a Type 3 projection cell in figure 8B (large arrow) and also can be seen distributed around processes of the DONdm projection cells (Fig. 8B, between small arrows). The photomicrograph also shows that there were no GABA-IR somata among this group of diagonal cells in DONdm (Figs. 8A,C). Only one horizontally oriented, double-labeled soma was seen in DONdm in that tissue (not shown). Thus, DONdm projection cells appear to receive GABAergic inputs. The origin of those GABAergic inputs cannot be determined because none of the bouton-like structures were double-labeled. The GABAergic source could be other neurons within the ipsilateral DON, other ipsilateral nuclei, such as SOdor (see discussion), or another contralateral source.

Discussion

This study consisted of three related experiments. First, we evaluated the morphology of auditory cells in the dorsal DON to assess the diversity of cell types in the auditory subdivisions, DONdl and DONdm. Second, we used a monoclonal antibody to determine that GABA is present in the DON and at two sites that receive input from the dorsal DON, the SOdor and TS. Lastly, we confirmed that some of the cells with axons in the commissural tract (between the left and right dorsal DON) exhibit GABA immunoreactivity.

Neurobiotin-filled cells in the dorsal auditory region of the DON were classified into 6 “types” using an analysis of cell morphology based on soma shape and filled processes around the soma (Fig. 2; Table 1). Three-dimensional reconstructions were not attempted due to extensive overlap of processes and the resultant lack of confidence in tracing processes through adjacent sections. Given the lack of reconstruction, the cell types may not reflect the true diversity of DON cells. However, the categories are consistent with previous work. Highstein et al. (1992) described the cytoarchitecture of the DON in *O. tau* as a mixture of round, spindle, and multipolar cells. The spindle shape might include Types 2, 3, and 5 of the present study since

the three were distinguished primarily by their processes, which may not have been visible with the Kluver-Berrera counterstain used in the Highstein study. Bass et al. (2001) reported that spherical or teardrop shaped somata were retrogradely filled in both DONdm and DONdl after injection of tracer into the auditory midbrain of *O. beta*, although the majority of the projection cells were in DONdm.

Comparison of the distribution of cell types in the two divisions of the auditory DON (dm and dl) in this study revealed slight differences. The teardrop Type 3 cells represented the highest proportion of filled cells in DONdl. In DONdm, Type 2 (fusiform) and Type 3 were present in essentially equal proportions. Contralaterally, commissural projection cells that were filled retrogradely were most often Type 3 cells in both DONdm and DONdl. Type 2 cells and Type 1 cells also contribute to the commissural tract in both DONdm and DONdl Surprisingly, Type 5 cells were common in both divisions of the DON in the ipsilateral fills, but they were rare among the commissural projection cells. We conclude that multiple cell types may be involved in binaural auditory processing.

The methodology employed to label large numbers of cells limited the morphological study of the cell types in DON, particularly when compared to the detailed analyses conducted in the dorsolateral nucleus of a frog (Feng and Lin, 1996), the nucleus angularis (Soares and Carr, 2001) and nucleus magnocellularis of the barn owl (Koppl and Carr, 1997), and the divisions of the cochlear nucleus of mammals (e.g., Cant, 1992; Doucet and Ryugo, 1997) for which Golgi staining or intracellular injections of label were used to reveal the details of the processes. As discussed and illustrated in Grothe et al. (2004; see figures 10.2 – 10.4), similarities in the morphologies of cells in the auditory nuclei exist across species, and there are similarities in the physiology of auditory cells, but thus far, there are no strong correlations between cell morphology and physiology across species. However, for completeness, we will note that fusiform or bipolar cells similar to the Type 2 or Type 5 cells in the DON of toadfish are present at binaural sites in the ascending auditory pathway of other vertebrates, e.g., the dorsolateral nucleus in the frog (Feng and Lin, 1996). In mammals, similar bipolar neurons are found in the medial and lateral superior olives, which are sites of binaural comparisons along the ITD and IID pathways, respectively (reviewed by Schwartz, 1992, but also see Grothe, 2000).

The immunohistochemistry conducted in the toadfish brainstem confirmed that GABA is a neurotransmitter in the auditory pathway of a teleost fish. GABA immunoreactive puncta and bouton-like endings were present in the neuropil and around somata in both DONdl and DONdm. GABA-IR somata were scattered throughout DONdl, but rare or not present in DONdm. GABA-IR somata in DONdl appeared to be Types 1 and 3.

Since projection cells are found in both DONdm and DONdl (Edds-Walton and Fay, 2005b; Bass et al. 2000), commissural cells were identified by retrograde labeling with TMR-dextran inserted into the left DON. That tissue was also reacted with the GABA antibody and showed that some of the commissural projection cells in the DONdl were also GABA immunoreactive. In the right DONdm, the somata of the diagonal commissural projection cells were not GABA-IR, but GABA-ergic puncta were associated with the somata and processes of those Type 3 cells. Therefore, the response properties of Type 3 commissural projection cells in DONdm are likely to be modulated by GABA. The source of that GABAergic input to DONdm could be the ipsilateral or contralateral DONdl or descending input from the secondary octaval nucleus, SOdor, which also exhibited GABA-immunoreactivity.

GABA immunoreactivity was lightly present in the midbrain, with puncta and somata scattered throughout both the auditory NC and the lateral line NVL. Edds-Walton and Fay (2005b) described binaural responses in the torus semicircularis in which cells were excited by both lateral line stimulation (water movements) and auditory stimulation, but also binaural cells that

were inhibited by increasing levels of auditory stimulation. Recording-site label (small extracellular injections of neurobiotin) indicated that binaural cells could be in either NC or NVL, but the cells inhibited by auditory stimulation tended to be deep in the NVL. The relatively consistent distribution of GABA-immunoreactivity in the TS did not provide any additional insights into the potential role that GABA might play in binaural processing in the midbrain.

Directional sharpening is more common in the TS (> 80% of cells) than in the DON, and frequency tuning is also apparent, though the two processes do not appear to result from the same computational process since directional sharpening and frequency tuning are not correlated (Edds-Walton and Fay, 2005a). The TS is the site of massive convergence of bilateral inputs from the DONs and the secondary octaval populations (Edds-Walton and Fay, 2003, 2005b). Thus a complex interaction of excitatory and inhibitory inputs is likely.

Earlier studies showed that GABA was present in the central nervous system in other species of bony and cartilagenous fishes (e.g., Ekstrom et al.,1987; Maler and Mugnaini, 1994; Duman and Bodznick, 1996, 1997), so it was not surprising that GABA immunoreactivity was widespread in the central nervous system of toadfish. We did not attempt to evaluate all of the sites that were GABA-IR, focusing instead on the sites in which we have documented directional auditory responses. While this study confirms that GABA is present in the ascending auditory pathway of a teleost fish, we caution that the pattern may not be identical in other fishes. In the only other study to evaluate auditory sites, GABA was reported as lightly present in the DON of the silver eel (*Anguilla anguilla*), although it was heavily present in other sites in the brain (Medina et al., 1994). In toadfish, GABA immunoreactivity was more prevalent in the DON than in the TS. Similarly, a recent study comparing two species of frogs (*Rana catesbeiana* and *Xenopus laevis*) revealed differences in the relative density and distribution of immunopositive cells at a variety of sites (Hollis and Boyd, 2005). Therefore, the relative density and distribution of GABA immunoreactivity along the auditory pathway of other teleost fishes may be different from what we have found in *O. tau*.

There are several potential roles that GABA might play in auditory processing in toadfish, based on its role in sensory processing in other fishes. For example, GABA mediates inhibition in the electrosensory system, a sensory system that may have predated the auditory system early in the evolution of jawed vertebrates (Grothe et al., 2004). Berman and Maler (1998) discuss the evidence they and others have collected for GABA's role in gain control via granule cells (GC2), coincidence detection, and surround inhibition in nonbasilar pyramidal cells in the weakly electric fish, *Apteronotus leptorhynchus* (Shumway and Maler, 1989; Maler and Mugnaini, 1994). In the little skate (*Raja erinacea*), Duman and Bodznick (1997) documented the presence of a population of GABAergic commissural cells in the electrosensory dorsal nucleus. In addition to a role in common mode rejection of self-generated noise (Bodznick and Montgomery, 1992; Montgomery and Bodznick, 1993), Duman and Bodznick (1996, 1997) suggested that GABA could be involved in a variety of roles in coordination of bilateral comparisons, as in other vertebrates. We suggest that GABA could play a role in bilateral comparisons and computations for sound source localization by teleost fish.

Fay (2005) presented a model for bilateral comparisons of saccular input in toadfish that is equivalent to interaural level difference (ILD or IID) calculations. Due to the nonparallel orientation and directional responses of the two saccules, a unique combination of relative inputs from the right versus the left ear would result from sound sources located at different azimuths around the fish. The neural computation required could be as simple as a “difference” function: overall comparison of right versus left inputs. Each saccular afferent has a directional response with a best azimuth determined by the overall orientation of the saccule, and best elevation determined by individual hair cell orientation on the saccule. Equality of the input

from the left and right ear would occur only when a sound source was directly in front of or behind the fish, or anywhere in the mid-saggital plane. This is an ambiguity shared by humans and most other two-eared vertebrates (Wightman and Kistler, 1993).

As noted in Grothe et al. (2004) and Carr and Edds-Walton (2008), despite differences in the periphery and the organization of the medullary nuclei, the basic ascending auditory pathway is remarkably similar among vertebrates. Determining the computational basis for sound source localization by teleosts may provide insight into commonalities of sound source localization among vertebrates.

The anatomical and immunohistochemical data collected during this study extend work published previously on the auditory circuit in the toadfish. The two known auditory divisions of the DON, DONdm and DONdl, have a similar assortment of cell types. Both divisions contribute to the commissural tract that is the basis for binaural processing in the DON, as confirmed physiologically by Edds-Walton and Fay (2009). Differences in GABA immunoreactivity indicate the two divisions may have different roles in the ascending circuit. Evaluation of the results of injections of GABA receptor blockers or antagonists at physiologically characterized sites in the dorsal DON and TS should reveal whether the directional (and frequency) response characteristics of auditory cells are mediated by GABA in a teleost fish.

Acknowledgments

Louie Kerr and Blair Rossetti provided instruction on the use of the Zeiss AxioImager (Z1), and Becky MacDonald provided instruction in photographing fluorescent images on the Z1 (at the Marine Biological Laboratory). Rudi Rottenfusser obtained appropriate filters for the Z1 for use with the fluorophores chosen for this project. Jeff Johnson (and members of the Federicci lab) at UC Riverside graciously allowed PLEW to use the Leica fluorescent microscope for tissue review and photography. Dr. Ewa Kukielka and Rosemary Lang in the Martinelli-Holstein lab provided technical assistance in the initial experiments that produced the successful protocol for the GABA immunohistochemistry. As has been the case throughout the 14+ years of our research at the MBL, the toadfish were obtained through the efforts of the excellent staff at the Marine Resources Center. We also thank the colleagues who read and contributed comments on an earlier version of this manuscript. This work was funded by grants from the National Institute for Deafness and Other Communication Disorders: DC006677 (GRH) and DC006215 (RRF).

References

Bass AH, Bodnar DA, Marchaterre MA. Midbrain acoustic circuitry in a vocalizing fish. J Comp Neurol 2000;419:505–531. [PubMed: 10742718]

Bass AH, Bodnar DA, Marchaterre MA. Acoustic nuclei in the medulla and midbrain of the vocalizing gulf toadfish (*Opsanus beta*). Brain Behav Evol 2001;57:63–79. [PubMed: 11435667]

Berman NJ, Maler L. Inhibition evoked from primary afferents in the electrosensory lateral line lobe of the weakly electric fish (*Apteronotus leptorhynchus*). J Neurophysiol 1998;80:3173–3196. [PubMed: 9862915]

Bodznick D, Montgomery JC. Suppression of ventilatory reafferance in the elasmobranch electrosensory system: medullary neuron receptive fields support a common mode rejection mechanism. J Exp Biol 1992;171:127–137.

Bruckner S, Hyson RL. Effect of GABA on the processing of interaural time differences in nucleus laminaris neurons in the chick. European J Neurosci 1998;10:3438–3450. [PubMed: 9824457]

Cant, NB. The cochlear nucleus: neuronal types and their synaptic organization. In: Webster, DB.; Popper, AN.; Fay, RR., editors. The Mammalian Auditory Pathway: Neuroanatomy. Springer Verlag; New York: 1992. p. 66-116.

Carr, CE.; Edds-Walton, PL. Vertebrate auditory pathways. In: Basbaum, AI.; Kaneko, A.; Shepherd, GM.; Westheimer, G., editors. The Senses: A Comprehensive Reference. Vol. 3. Academic Press; San Diego: 2008. p. 499-524.Audition, Dallos P., Oertel D.

Carr CE, Fujita I, Konishi M. Distribution of GABAergic neurons and terminals in the auditory system of the barn owl. J Comp Neurol 1989;286:190–207. [PubMed: 2794115]

Doucet JR, Ryugo DK. Projections from the ventral cochlear nucleus to the dorsal cochlear nucleus in rats. J Comp Neurol 1997;385:245–264. [PubMed: 9268126]

Duman CH, Bodznick D. A role for GABAergic inhibition in electrosensory processing and common mode rejection in the dorsal nucleus of the little skate, *Raja erinacea*. J Comp Physiol 1996;179:797–807. [PubMed: 8956498]

Duman CH, Bodznick D. Distinct but overlapping populations of commissural and GABAergic neurons in the dorsal nucleus of the little skate, *Raja erinacea*. Brain, Behav Evol 1997;49:99–109. [PubMed: 9031733]

Edds-Walton PL. Anatomical evidence for binaural processing in the descending octaval nucleus of the toadfish (*Opsanus tau*). Hear Res 1998;123:41–54. [PubMed: 9745954]

Edds-Walton PL, Fay RR. Directional auditory responses in the descending octaval nucleus of the toadfish (*Opsanus tau*). Biol Bull 1998;195:191–192. [PubMed: 9818363]

Edds-Walton PL, Fay RR. Directional selectivity and frequency tuning of midbrain cells in the oyster toadfish, *Opsanus tau*. J Comp Physiol A 2003;189:527–543.

Edds-Walton PL, Fay RR. Sharpening of directional responses along the auditory pathway of the oyster toadfish, *Opsanus tau*. J Comp Physiol A 2005a;191:1079–1086.

Edds-Walton PL, Fay RR. Projections to bimodal sites in the torus semicircularis of the toadfish, *Opsanus tau*. Brain, Behav Evol 2005b;66:73–87. [PubMed: 15914974]

Edds-Walton PL, Fay RR. Directional and frequency response characteristics in the descending octaval nucleus of the toadfish (*Opsanus tau*). J Comp Physiol A 2008;194:1013–1029.

Edds-Walton PL, Fay RR. Physiological evidence for binaural directional computations in the brainstem of the oyster toadfish, *Opsanus tau* (L.). J Exper Biol 2009;212(10):1483–1493. [PubMed: 19411542]

Edds-Walton PL, Popper AN. Hair cell orientation patterns on the saccules of juvenile and adult toadfish, *Opsanus tau*. Acta Zool 1995;76:257–265. [PubMed: 11539851]

Edds-Walton PL, Fay RR, Highstein SM. Dendritic arbors and central projections of physiologically characterized auditory fibers from the saccule of the toadfish, *Opsanus tau*. J Comp Neurol 1999;411:212–238. [PubMed: 10404249]

Ekstrom P, Van Veen T, Bruum A, Ehing B. GABA-immunoreactive neurons in the photosensory pineal organ of the rainbow trout: two distinct neuronal populations. Cell Tissue Res 1987;250:87–92. [PubMed: 3652169]

Fay, RR. Sound source localization by fishes. In: Popper, AN.; Fay, RR., editors. Sound Source Localization. Springer; New York: 2005. p. 36-66.Springer Handbook of Auditory Research, vol. 25

Fay RR, Edds-Walton PL. Directional response properties of saccular afferents of the toadfish, *Opsanus tau*. Hear Res 1997;111:1–21. [PubMed: 9307307]

Fay RR, Edds-Walton PL. Sharpening of directional auditory input in the descending octaval nucleus of the toadfish, *Opsanus tau*. Biol Bull 1999;197:240–241. [PubMed: 10573842]

Feng AS, Lin WY. Neuronal architecture of the dorsal nucleus (cochlear nucleus) of the frog, *Rana pipiens pipiens*. J Comp Neurol 1996;366:320–334. [PubMed: 8698890]

Fish, JF. The effect of sound playback on the toadfish. In: Winn, HE.; Olla, BW., editors. Behavior of Marine Animals. Vol. 2. Plenum Press; New York: 1972. p. 386-434.

Funabiki K, Koyano K, Ohmori H. The role of GABAergic inputs for coincidence detection in the neurons of nucleus laminaris of the chick. J Physiol 1998;508(3):851–869. [PubMed: 9518738]

Gray G, Winn HE. Reproductive ecology and sound production of the toadfish, *Opsanus tau*. Ecology 1961;42:274–282.

Grothe B. The evolution of temporal processing in the medial superior olive, an auditory brainstem structure. Prog Neurobiol 2000;61:581–610. [PubMed: 10775798]

Grothe, B.; Carr, CE.; Casseday, JH.; Fritzsch, B.; Koppl, C. The evolution of central pathways and their neural processing patterns. In: Manley, GA.; Popper, AN.; Fay, RR., editors. Evolution of the Vertebrate Auditory System. Springer; New York: 2004. p. 289-359.

Hancock MB. A serotonin immunoreactive fiber system in the dorsal column of the spinal cord. Neurosci Lett 1982;31:247–252. [PubMed: 6752764]

Highstein SM, Kitch R, Carey J, Baker R. Anatomical organization of the brainstem octavolateralis area of the oyster toadfish, *Opsanus tau*. J Comp Neurol 1992;319:501–518. [PubMed: 1619042]

Holstein GR, Martinelli GP, Henderson SC, Friedrich VL Jr, Rabbitt RD, Highstein SM. Gamma-aminobutyric acid is present in a spatially discrete subpopulation of hair cells in the crista ampullaris of the toadfish *Opsanus tau*. J Comp Neurol 2004a;471:1–10. [PubMed: 14983471]

Holstein GR, Rabbitt RD, Martinelli GP, Friedrich VL Jr, Boyle RD, Highstein SM. Convergence of excitatory and inhibitory hair cell transmitters shapes vestibular afferent responses. Proc Natl Acad Sci USA 2004b;101:15766–15771. [PubMed: 15505229]

Hollis DM, Boyd SK. Distribution of GABA-like immunoreactive cell bodies in the brains of two amphibians, *Rana catesbeiana* and *Xenopus laevis*. Brain, Behav Evol 2005;65:127–142. [PubMed: 15627724]

Horner K, Sand O, Enger PS. Binaural interaction in the cod. J Exp Biol 1980;85:323–331.

Hyson RL. The analysis of interaural time differences in the chick brain stem. Physiol Behav 2005;86:297–305. [PubMed: 16202434]

Hyson RL, Reyes AD, Rubel EW. A depolarizing inhibitory response to GABA in brainstem auditory neurons of the chick. Brain Res 1995;677:117–126. [PubMed: 7606455]

Klug A, Park TG, Pollak GD. Glycine and GABA influence binaural processing in the inferior colliculus of the mustache bat. J Neurophysiol 1995;74(4):1701–1713. [PubMed: 8989406]

Konishi M. Coding of auditory space. Ann Rev Neurosci 2003;26:31–55. [PubMed: 14527266]

Koppl C, Carr CE. Low-frequency pathway in the barn owl's auditory brainstem. J Comp Neurol 1997;378:265–282. [PubMed: 9120065]

Maler L, Mugnaini E. Correlating gamma-aminobutyric acid circuits and sensory function in the electrosensory lateral line lobe of a gymnotiform fish. J Comp Neurol 1994;345:224–252. [PubMed: 7523460]

McCormick, CA. Anatomy of the central auditory pathways of fish and amphibians. In: Popper, AN.; Fay, RR., editors. Comparative Hearing: Fish and Amphibians. Springer; New York: 1999. p. 155-217.

Medina M, Reperant J, Dufour S, Ward R, Le Belle N, Miceli D. The distribution of GABA-immunoreactive neurons in the brain of the silver eel (*Anguilla anguilla* L.). Anat Embryol 1994;189:25–39. [PubMed: 8192235]

Mensinger AF, Carey JP, Boyle R, Highstein SM. Differential central projections of physiologically characterized horizontal semicircular canal vestibular nerve afferents in the toadfish, *Opsanus tau*. J Comp Neurol 1997;384:71–85. [PubMed: 9214541]

Montgomery JC, Bodznick D. Hindbrain circuitry mediating common mode suppression of ventilatory reafference in the electrosensory system of the little skate *Raja erinacea*. J Exp Biol 1993;183:203–215.

Muller CM. Gamma-aminobutyric acid immunoreactivity in brainstem auditory nuclei of the chicken. Neurosci Lett 1987;77:272–276. [PubMed: 3302766]

Park TJ, Pollak GD. GABA shapes sensitivity to interaural intensity disparities in the mustache bat's inferior colliculus: implications for encoding sound location. J Neurosci 1993;13:2050–2067. [PubMed: 8478690]

Park TJ, Pollak GD. Azimuthal receptive fields are shaped by GABAergic inhibition in the inferior colliculus of the mustache bat. J Neurophys 1994;72(2):1080–1090.

Pollak GD, Burger RM, Park TJ, Klug A, Bauer EE. Roles of inhibition for transforming binaural properties in the brainstem auditory system. Hear Res 2002;168(1-2):60–78. [PubMed: 12117510]

Pollak GD, Burger RM, Klug A. Dissecting the circuitry of the auditory system. Trends in Neurosci 2003;26(1):33–39.

Popper, AN.; Fay, RR. The auditory periphery in fishes. In: Fay, RR.; Popper, AN., editors. Comparative Hearing: Fish and Amphibians. Springer; New York: 1999. p. 43-100.

Schwartz, IR. The superior olivary complex and lateral lemniscal nuclei. In: Webster, DB.; Popper, AN.; Fay, RR., editors. The Mammalian Auditory Pathway: Neuroanatomy. Springer-Verlag; New York: 1992. p. 117-167.

Shumway CA, Maler L. GABAergic inhibition shapes temporal and spatial response properties of pyramidal cells in the electrosensory lateral line lobe of gymnotiform fish. J Comp Physiol A 1989;164:391–407. [PubMed: 2709342]

Soares D, Carr CE. The cytoarchitecture of the nucleus angularis of the barn owl (*Tyto alba*). J Comp Neurol 2001;429:192–205. [PubMed: 11116214]

Winn, HE. Vocal facilitation and the biological significance of toadfish sounds. In: Tavolga, WN., editor. Marine Bioacoustics. Vol. 2. Pergamon Press; Oxford: 1967. p. 15-43.

Wightman, FL.; Kistler, DJ. Sound localization. In: Yost, WA.; Popper, AN.; Fay, RR., editors. Human Psychophysics. Springer-Verlag; New York: 1993. p. 155-192.

Abbreviations

CC	crista cerebellaris
DON	descending octaval nucleus (entire)
DONdl	dorsolateral division of the DON
DONdm	dorsomedial division of the DON
DONvl	dorsolateral division of the DON
GABA	gamma aminobutyric acid, neurotransmitter
GABA-IR	GABA immunoreactive
IID	interaural intensity difference
ITD	interaural time difference
MAb	monoclonal antibody
NA	nucleus angularis (in avians)
NC	nucleus centralis, in TS
NGS	normal goat serum
NVL	nucleus ventrolateralis, in TS
PBS	phosphate buffered saline
SOdor	dorsal division of the secondary octaval population
TMR	tetramethyl rhodamine
TS	torus semicircularis, midbrain
ven	ventricle
Vdesc	descending trigeminal (V_d) tract
VII	cranial nerve (facial nucleus)
VIII	cranial nerve (acoustic)

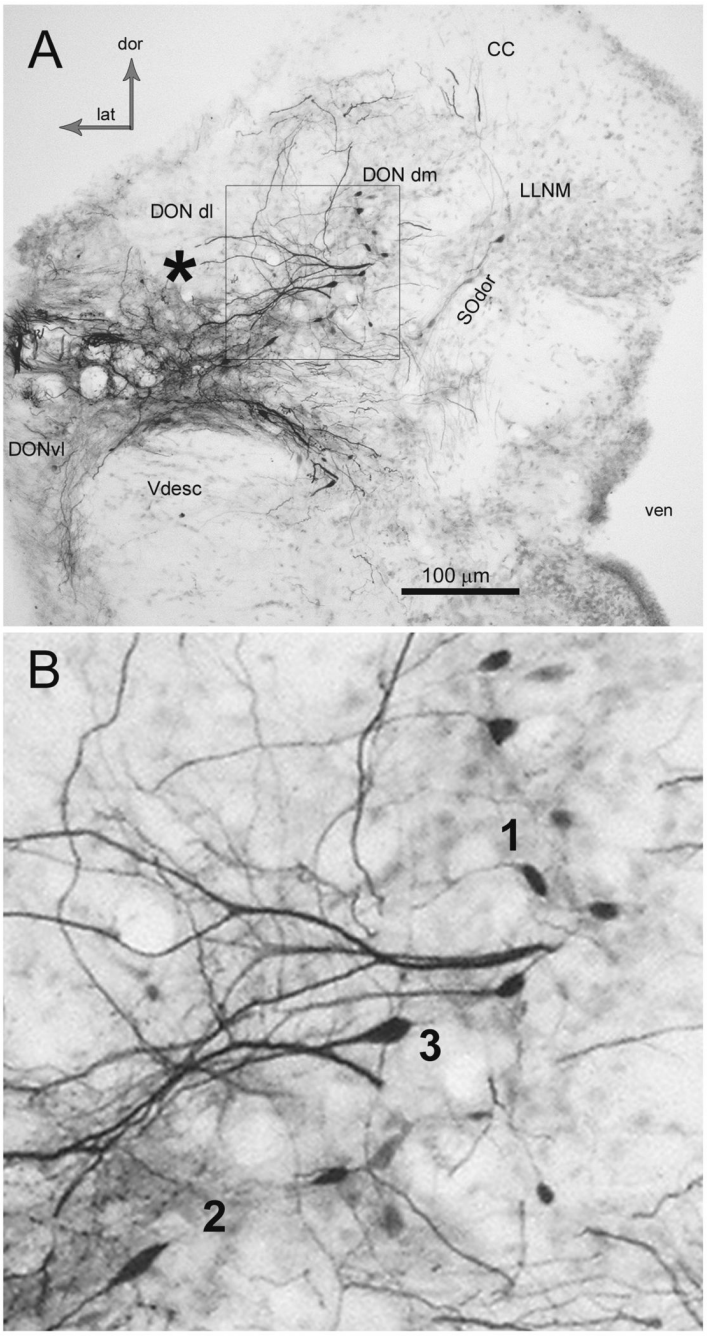

Figure 1.

Photomicrograph of coronal section (50 μm) through the rostral descending octaval nucleus (DON) illustrating results of a large neurobiotin injection. ***A***. The asterisk indicates area where label was injected extracellularly into the left, dorsolateral division (DONdl), although the actual injection site is not in this section. Note the filled processes and somata of cells in the dorsomedial division (DONdm). Relatively pale labeling of the diagonal cell group in the dorsal division of the secondary octaval population (SOdor) is also present. The box in A is enlarged in B. CC, cerebellar crest; DONvl, ventrolateral DON; dor, dorsal; lat, lateral; LLNM, lateral line nucleus medialis; Vdesc descending tract of trigeminal; ven, ventricle. ***B***. Cells in DONdm that took up neurobiotin injected extracellularly (enlarged image of box in A). Note the lateral

processes that extend into the DONdl. Three morphologies are distinguishable in this image, indicated by numerals adjacent to the somata. The numerals correspond to the cell types presented in the text and in the drawings in Figure 2.

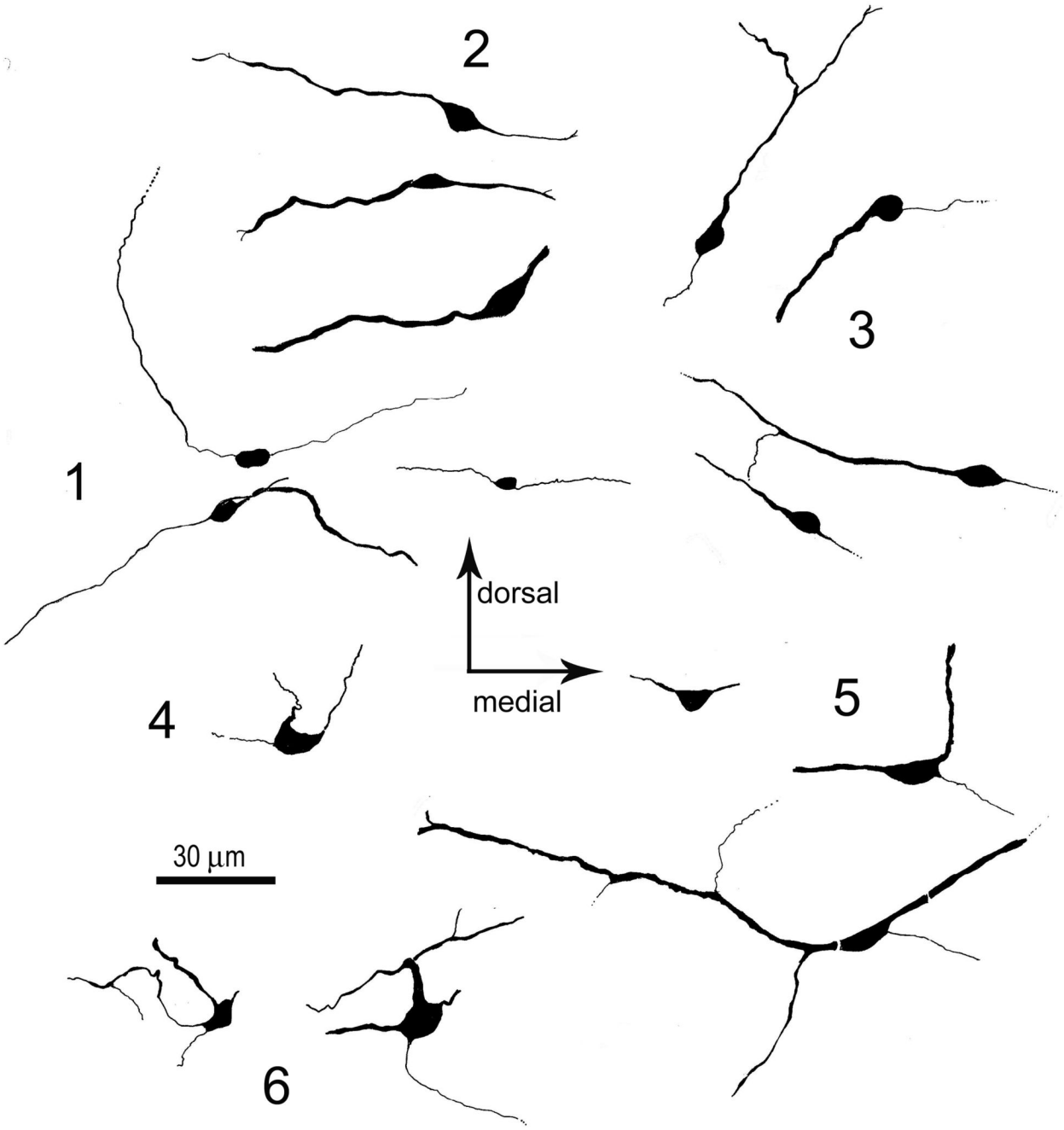

Figure 2.
Drawings of the cell types filled with neurobiotin ipsilateral to the injection site. The numbers 1-6 correspond to the morphologic cell types referred to in the text. Type 4 showed little variation and is represented by one drawing. All cells shown are oriented similarly with regard to dorsal and medial, as indicated.

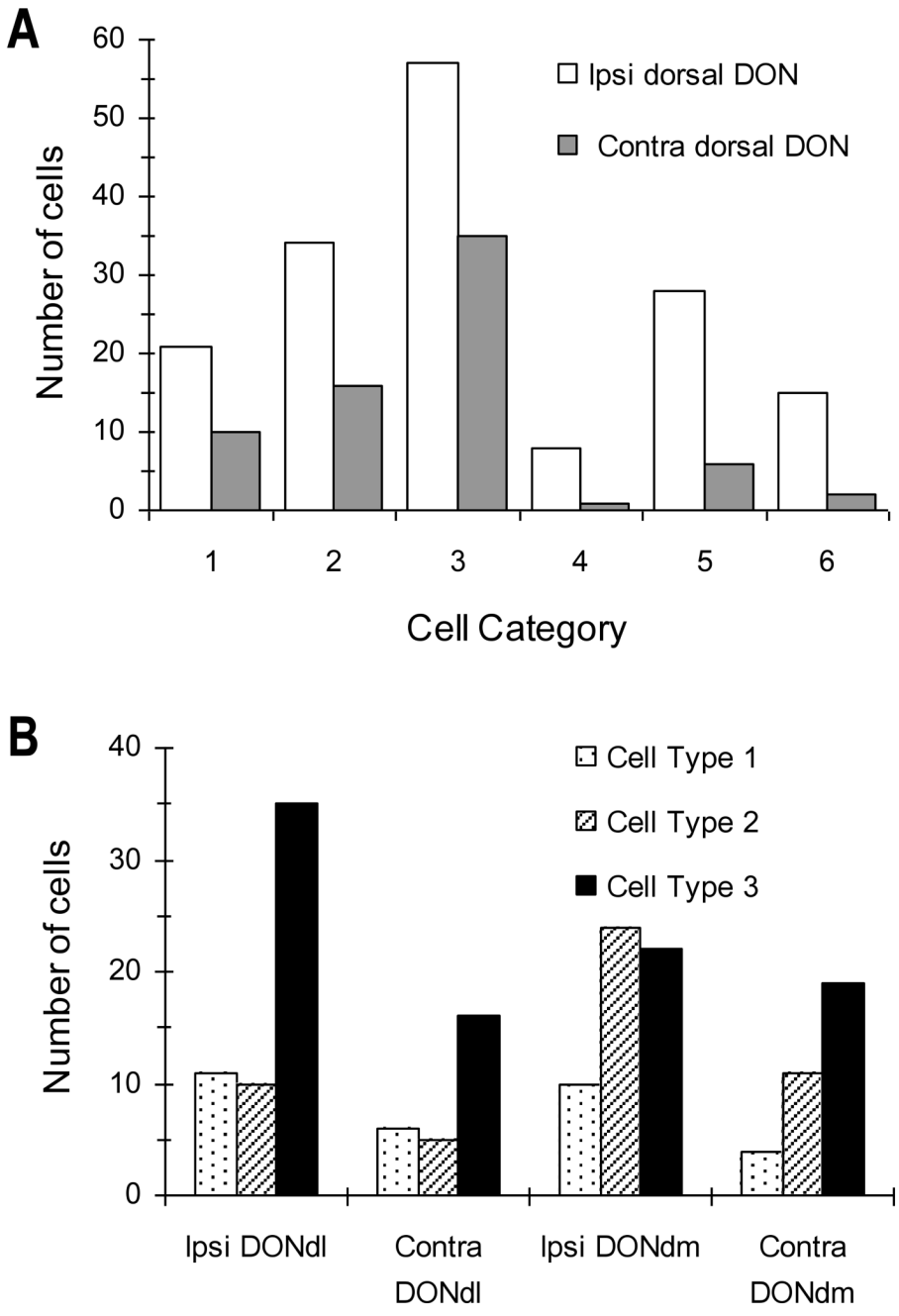

Figure 3.

Cell types labeled with neurobiotin in the dorsal DON in brains with bilateral fills: ipsilateral n = 163; contralateral n = 70.

A. The number of cell morphology Types 1 – 6 filled ipsilaterally and contralaterally. Note that fewer cells in each category were filled contralaterally.

B. Comparison of the number of Types 1 - 3 filled with neurobiotin in dorsolateral (dl) versus dorsomedial (dm) sites in the DON ipsilaterally and contralaterally.

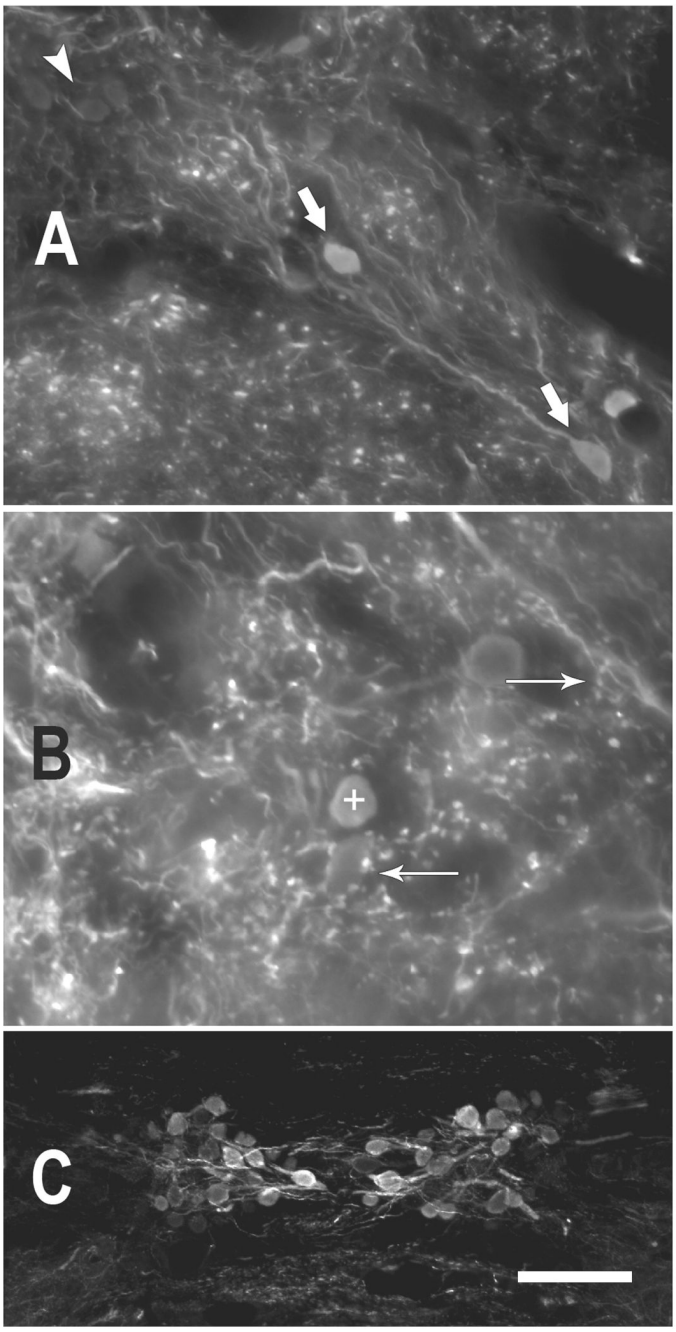

Figure 4.

Photomicrographs illustrating GABA immunoreactivity in the toadfish. ***A***. GABA immunoreactive somata and processes in dorsal DON. GABA-negative somata (white arrowhead, upper left) are lightly visible due to autofluorescence, but were clearly differentiated from the GABA-immunoreactive somata (large white arrows). (coronal, 50 μm section) ***B***. GABA-positive puncta surround GABA-negative somata (e.g., arrow pointing left) and are present in the neuropil of the DON. Sometimes the puncta occur in sprays (arrow pointing right) that appeared to bear multiple boutons from the same process. The + symbol marks a GABA-positive soma (dorsal DON, coronal, 25 μm section). *C*. The rostral efferent nucleus of cranial VIII illustrates a range of immunoreactivity among those somata. (25 μm

horizontal section) More heavily GABA-IR somata are more medial (near the midline of the section). (scale bar in C = 25 μm for A,B and 100μm for C)

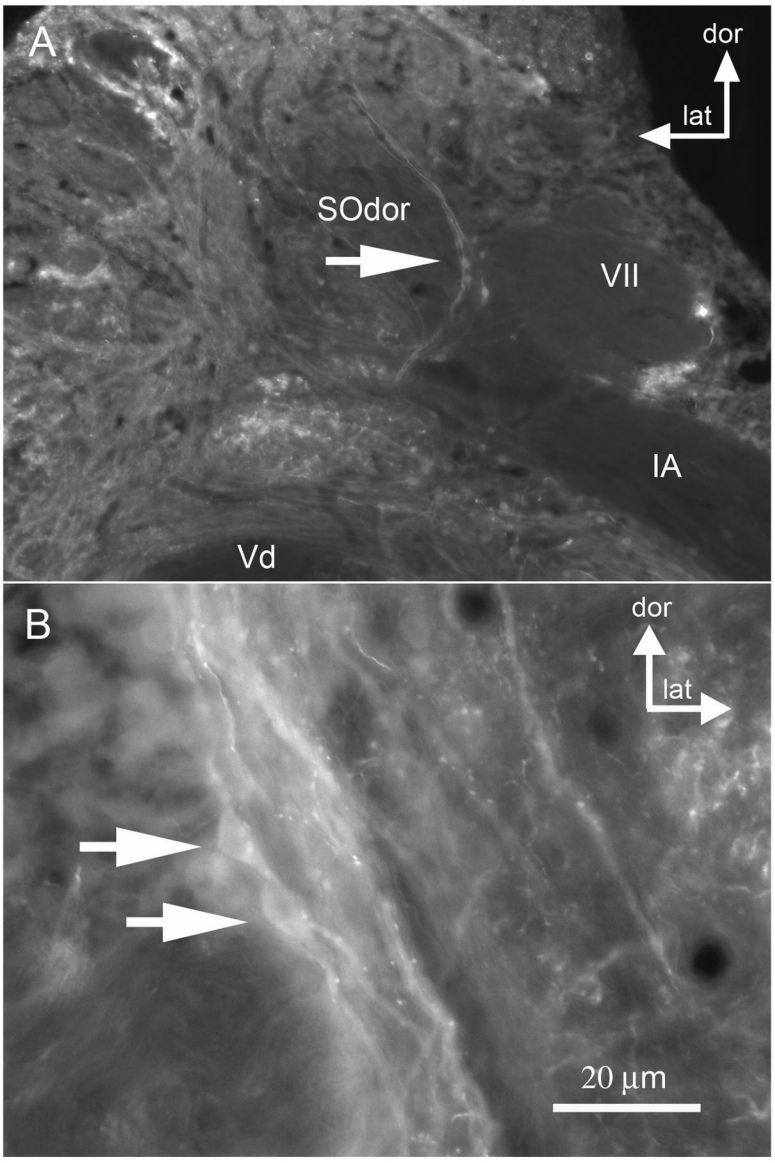

Figure 5.
Photomicrographs illustrating GABA immunoreactivity in the dorsal division of the secondary octaval population (SOdor). ***A***. Putative GABA-IR cells in the left SOdor are indicated by the large arrow (coronal section). ***B***. The right SOdor in same toadfish, indicating GABA-IR somata (two arrows) and puncta. [other abbreviations: dor dorsal, lat lateral, Vd descending tract of trigeminal; VII sensory facial; IA internal arcuate tract]

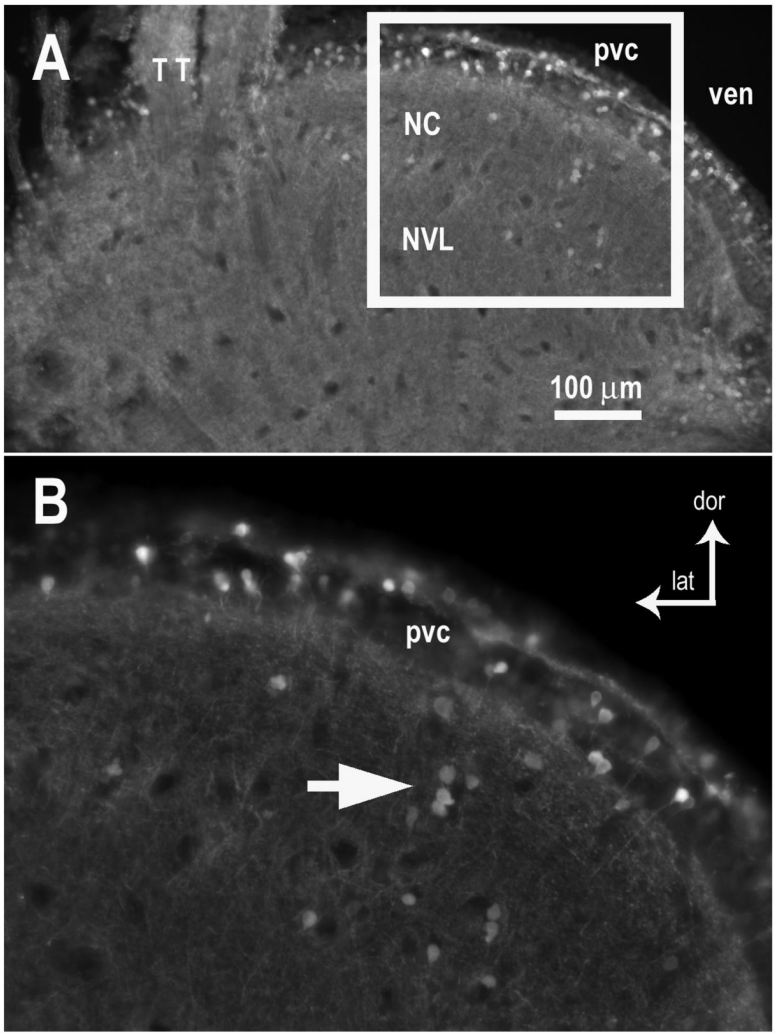

Figure 6.

GABA immunoreactivity in the midbrain torus semicircularis of the toadfish. ***A***. Both the auditory nucleus centralis (NC) and the nucleus ventrolateralis (NVL, which receives input from lateral line nucleus medialis) contained GABA-IR somata and puncta throughout the neuropil. Overlying the NC is a periventricular cell layer (pvc), which appears to have a high proportion of GABA-IR somata. ***B***. Enlarged area shown in white box in A. White arrow indicates a small group of GABA-IR somata in NC. GABA-IR somata are scattered among GABA-negative somata in the periventricular cell layer. Coronal sections (50 μm). [other abbreviations: dor dorsal, lat lateral, TT tectal tract, ven ventricle]

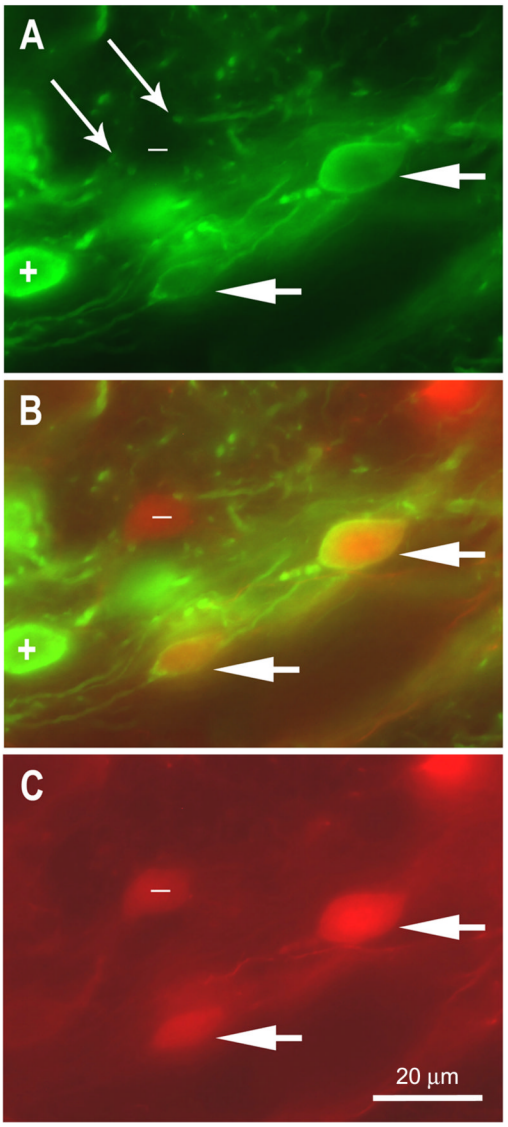

Figure 7.

Photomicrograph of coronal section in dorsolateral DON in which tetramethyl rhodamine dextran (TMR, red) was used to label commissural projection cells and the tissue was reacted with GABA93 MAb with Alexa 488 secondary antibody (green). The plane of focus is the same for A – C. (50 μm section). ***A***. GABA-IR soma (e.g., + symbol), processes, and puncta are apparent. Paired thin arrows indicate GABA-IR processes in proximity of fusiform GABA-negative soma (labeled with – symbol). Short arrows indicate two projection cells that are double labeled (compare to merged image in B and to C). ***B***. Merged image of A and C illustrates GABA-IR soma (+ symbol), GABA-negative commissural projection cell (- symbol), and commissural projection cells that are GABA-IR (short arrows). ***C***. TMR-dextran placed in the left DON retrogradely filled these commissural projection cells in the right DONdl. The symbols and arrows are consistent with those used in A and B.

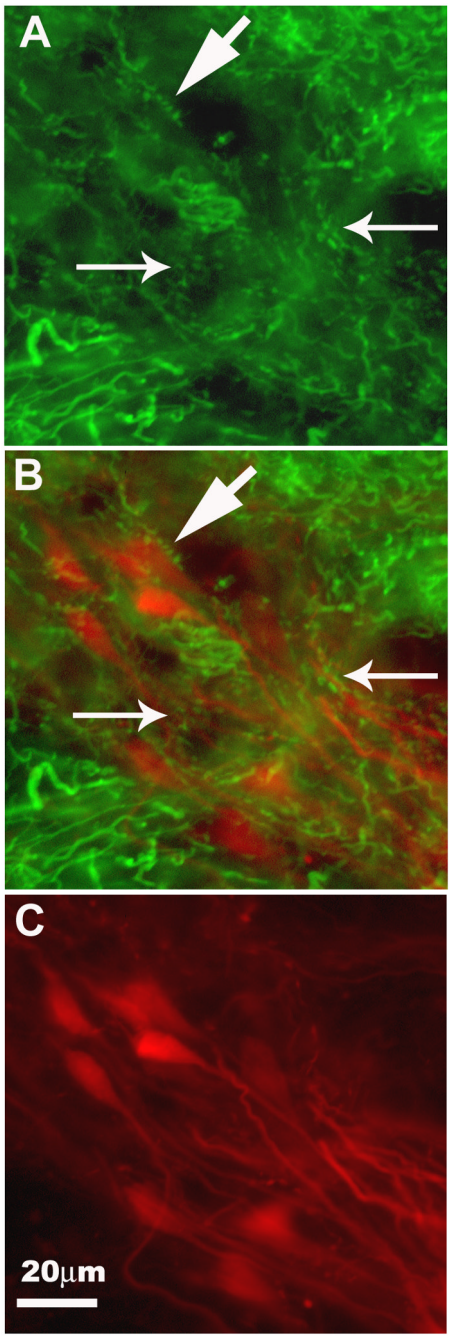

Figure 8.

GABAergic inputs to projection cells in the dorsomedial DON (DONdm). The same coronal section (25 μm) is shown in each panel. ***A***. GABA-IR fibers and puncta in neuropil (small arrows) and around GABA-negative somata (e.g., large arrow). ***B***. Merged image of A and C. GABA-IR puncta can be seen along the soma (large arrow) and large processes (between small arrows) of TMR-dextran filled projection cells in the DONdm. ***C***. DONdm projection cells viewed with TMR filter only. This diagonally oriented cell group (all Type 3) was filled retrogradely via their projections to the contralateral DON. [dorsal is up, medial is left]

Table 1

Ranges of morphological measurements of DON somata filled with neurobiotin.[1]

Cell Type	Long axis (μm) range (mode)	Short axis[2] (μm) range (mode)
1 (n = 35)	6 – 15 (10)	5 – 11 (8)
2 (n = 48)	8 – 25 (15)	5 – 18 (7)
3 (n = 84)	6 – 20 (10)	5 – 16 (8)
4 (n = 11)	9 – 25 (15)	5 – 11 (10)
5 (n = 38)	9 – 22 (20)	5 – 15 (10)
6 (n = 17)	9 – 25 (15)	6 – 20 (10)

[1] measurements include only cells that were ipsilateral to the neurobiotin application; no adjustments were made for the effects of fixation and processing

[2] short axis was measured perpendicular to the long axis

Table 2

Morphological cell types labeled ipsilaterally following a neurobiotin injection in the dorsal DON. Data are presented by subdivisions of the auditory DON [dorsolateral (dl) and dorsomedial (dm)] to illustrate differences in distribution of the cell types in each (n = 10 fish). See text for description of cell morphology and Figure 2 for drawings.

Cell Type	Ipsilateral DONdl (n)	*% of dl*	Ipsilateral DONdm (n)	*% of dm*
1	21	*16*	14	*13*
2	18	*14*	29	*28*
3	56	*43*	28	*27*
4	9	*7*	1	*1*
5	17	*13*	23	*22*
6	8	*6*	9	*9*
Total:	**129**	*100%*	**104**	*100%*